THE FATIGUE BEHAVIOUR OF FRICTION STIR WELDED ALUMINIUM JOINTS




M. Gutensohn[1] G. Wagner[2] F. Walther[3] D. Eifler[4]

Institute of Materials Science and Engineering, University of Kaiserslautern (Germany)
E-mail: [1] gutensohn@mv.uni-kl.de, [2] gwagner@mv.uni-kl.de, [3] walther@mv.uni-kl.de, [4] eifler@mv.uni-kl.de

ABSTRACT

The friction stir welding (FSW) technology enables the production of high-strength joints of light weight metal sheets. In this paper, the fatigue properties of AA5454-FSW-joints will be discussed. High-resolution plastic strain amplitude, temperature and electrical resistance measurements were performed to describe and evaluate the fatigue behaviour in detail. The plastic strain amplitude determined in mechanical stress-strain hysteresis measurements is qualified to describe the proceeding fatigue damage. Additionally, the change in temperature caused by plastic deformation work and measured with thermocouples fixed on the specimen surface allows a precise fatigue assessment. The electrical resistance measurements are directly related to the fatigue-induced defect structure and density in the welding zone. The fatigue behaviour of the welding zone, which corresponds to the specimen gauge length, is characterized by pronounced cyclic hardening leading to a plastic strain amplitude nearby zero. Additionally, results of microscopic investigations of the welding zone are presented for a microstructure-related interpretation of the fatigue properties.

IIW-Thesaurus Keywords: *Aluminium alloys; Fatigue strength; Friction stir welding; Friction welding; Light metals; Microstructure; Mechanical properties; Reference lists.*

1 INTRODUCTION

In automotive and aircraft industry as well as for shipbuilding, weight reduction is a predominant aim of innovative products. For the integration of light weight metals in complex mechanical components friction stir welding is a suitable solid state joining technique. Since its development in 1991 [1], this process is more and more accepted in industrial manufacturing as an effective method to join light metals, such as aluminium or magnesium alloys [2, 3]. A friction stir weld is produced by plunging a rotating tool, consisting of a shoulder and a profiled pin into the assembly components. As the rotating tool moves along the joint line the material is deformed like in an extrusion process [4]. The considerable advantages of this innovative welding technique, such as low welding temperature and pore-free welding zone in the case of optimized welding parameters, lead to numerous industrial applications, which are described in [5-7]. For a further extension of the application fields of FSW, the knowledge of the cyclic deformation behaviour of such joints is necessarily required in addition to their monotonic properties. One major research field at the Institute of Materials Science and Engineering at the University of Kaiserslautern in Germany is the characterization of the fatigue behaviour of metals by using mechanical stress-strain hysteresis, temperature and electrical resistance measurement techniques

Doc. IIW-1878-07 (ex-doc. III-1437r1-07) recommended for publication by Commission III “Resistance welding, solid state welding and allied joining processes”.

[8-10]. The main topic of this paper is the application of these methods to describe the fatigue behaviour of friction stir welded aluminium alloys.

2 EXPERIMENTAL PROCEDURE

2.1 Material

The investigations were carried out with the aluminium wrought alloy AA5454 (Table 1). Besides the corrosion behaviour, the manganese and chromium fraction particularly improves the monotonic and cyclic strength [11].

The aluminium alloy was welded in the condition H22, that means rolled and annealed to a hardness of 100 HV10. Because of its pronounced ductility in this condition, AA5454 is often used for cupping components in automotive industry.

The microstructure of the AA5454 sheets is shown in a light micrograph in Figure 1. The microstructure consists of an intermetallic Al-Mg-phase (β-phase) embedded in an aluminium solution α-phase. Both phases are elongated in longitudinal direction due to the rolling process.

In monotonic tensile tests a yield strength $R_{p0.2}$ of about 220 MPa, a tensile strength R_m of 300 MPa and an elongation after fracture A of 8 % were measured for the sheet metal in rolling direction.

2.2 Experimental procedures

The AA5454 sheets, with the dimensions of 125 x 300 x 3.5 mm³, were butt welded perpendicular to the rolling direction of the sheets by using a standard milling machine and a standard tool geometry with a shoulder diameter of approximately 15 mm and a M3.5 pin. The machine is supplemented by a measurement unit to record temperatures and welding forces online during the FSW process. The temperature in the welding zone was measured by thermocouples implemented along the seam.

In systematic investigations, the welding process was optimized with regard to attain high tensile strengths of the FSW joints. The investigations show that 1 500 rpm tool revolutions and a feed rate of 200 mm/min are best suited to produce pore-free and high strength welds. After welding, the sheets were cut, milled and polished for the monotonic and cyclic investigations according to the details in Figure 2.

To receive information exclusively from the area of the welding zone, the gauge length for the monotonic and cyclic investigations was 15 mm corresponding to the diameter of the shoulder of the welding tool.

In order to characterize the fatigue behaviour of AA5454-FSW-joints, axial stress-controlled constant amplitude tests were performed according to ISO 1099 standard with a load ratio of R = 0 at ambient temperature using a frequency of f = 5 Hz and triangular waveforms.

The experimental setup for the fatigue tests is shown in Figure 3. The plastic strain amplitude $\varepsilon_{a,p}$ is measured with an extensometer. Four thermocouples fixed on the specimen surface allow highly accurate temperature measurements. The local temperatures T_1, T_2 and T_3

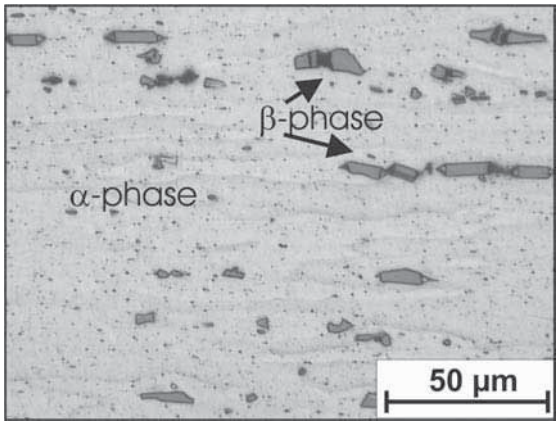

↔ *rolling direction*

Figure 1 – Light micrograph of AA5454 base material

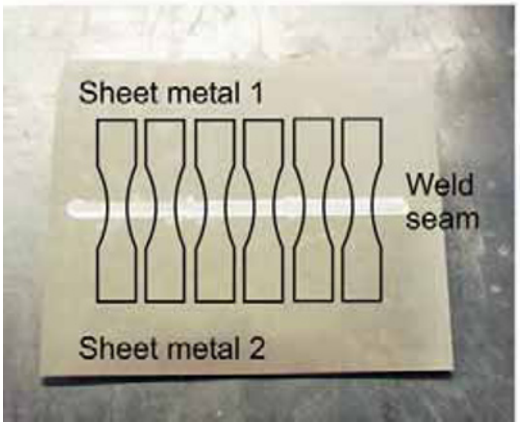

a) Positions of specimen extraction

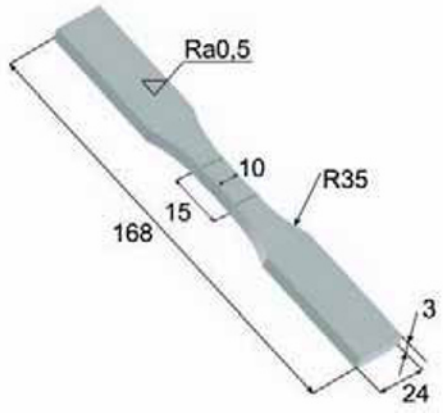

b) Specimen geometry

Figure 2

Table 1 – Chemical composition of AA5454

(wt-%)	Mg	Mn	Fe	Si	Zn	Ti	Cr	Cu
AA5454	2.85	0.84	0.31	0.13	0.01	0.01	0.08	0.03

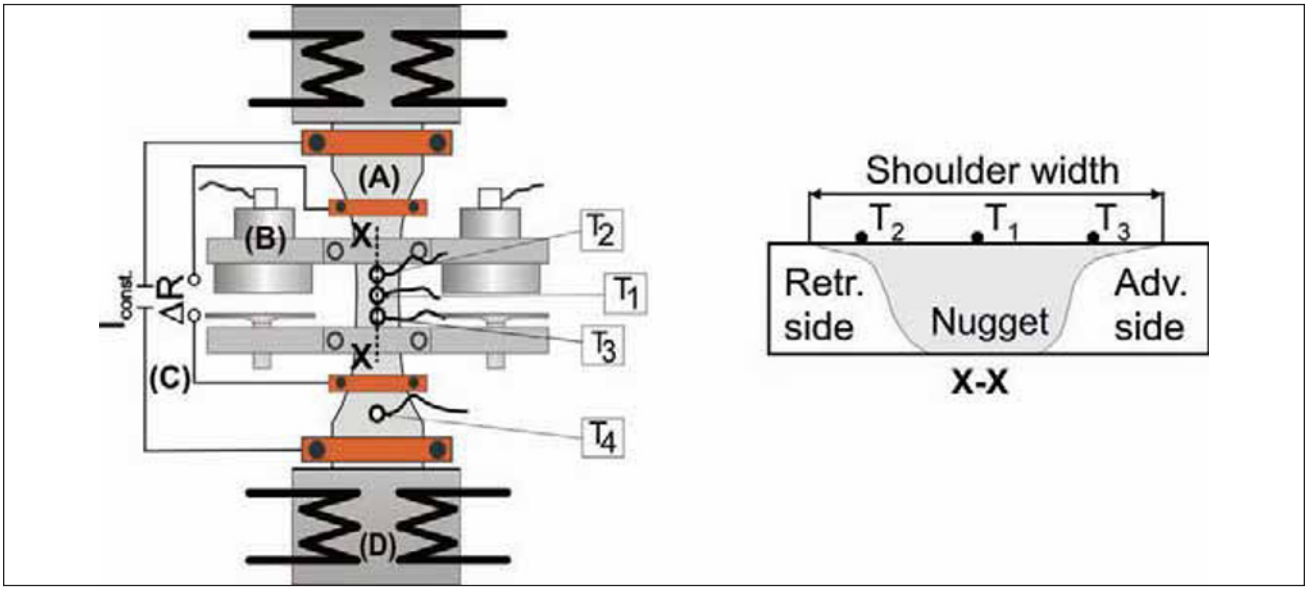

(A) Specimen
(B) Extensometer
(C) Electrical resistance measurement
(D) Thermostatically-controlled hydraulic grips
T_1-T_4 Thermocouples

a) Experimental setup **b) Section X-X of the specimen gauge length**

Figure 3

were measured in the gauge length between the extensometer clamps, T_1 at the weld nugget in the middle of the joint, T_2 at the retreating side and T_3 at the advancing side of the joint (Figure 3). The cross-section at the measurement position of T_4 is significantly larger compared to the cross-section of the gauge length, where T_1, T_2 and T_3 are measured. Consequently, the deformation at T_4 is completely elastic and the temperature T_4 could be used as a reference value to evaluate the temperature increase due to cyclic plastic deformation at the positions T_1, T_2 and T_3.

Using the following equation Eq. (1), thermal influences from the environment can be eliminated:

$$\Delta T_n = (T_n - T_4) \text{ with } n = 1, 2, 3 \quad (1)$$

The change in specimen temperature is caused by energy dissipation as a consequence of plastic deformation in the gauge length [12]. For the electric resistance measurements a DC power supply was fixed at both specimen shafts. The change in voltage, which directly corresponds to the electrical resistance ΔR was measured between the gauge length and the shafts. Temperature and electrical resistance measurements are not related to a defined gauge length and allow a non-destructive evaluation of a proceeding fatigue damage in the volume part influenced by the welding process [13].

3 RESULTS

3.1 Welding process

Before the welding process was started, three thermocouples $T_{S1\text{-}S3}$ were positioned in the butt-line at the starting point, in the middle and at the end of the weld seam (S). In Figure 4 characteristic force and temperature developments during the welding process are shown. After a short peak at the beginning of the welding the axial welding force increases slowly from 6 200 N to 6 800 N along the weld seam as a result of a position controlled welding process. The temperature rises and the maximum temperature of about 530 °C for each measuring point is almost identical along the whole seam. The investigations clearly show, that the maximum welding temperature never reaches the melting temperature of the AA5454 which is 645 °C.

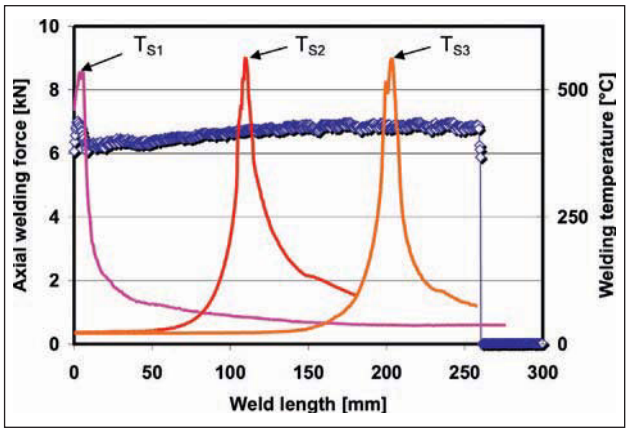

Figure 4 – Axial welding force and welding temperature during FSW of AA5454

3.2 Microstructure

The cross section of a friction stir welded AA5454-joint (Figure 5) shows characteristic microstructural changes. In the middle of the butt weld [Figure 5 c)] the FSW nugget with a typical onion ring structure is visible [14]. The nugget is characterized by a fine grain structure

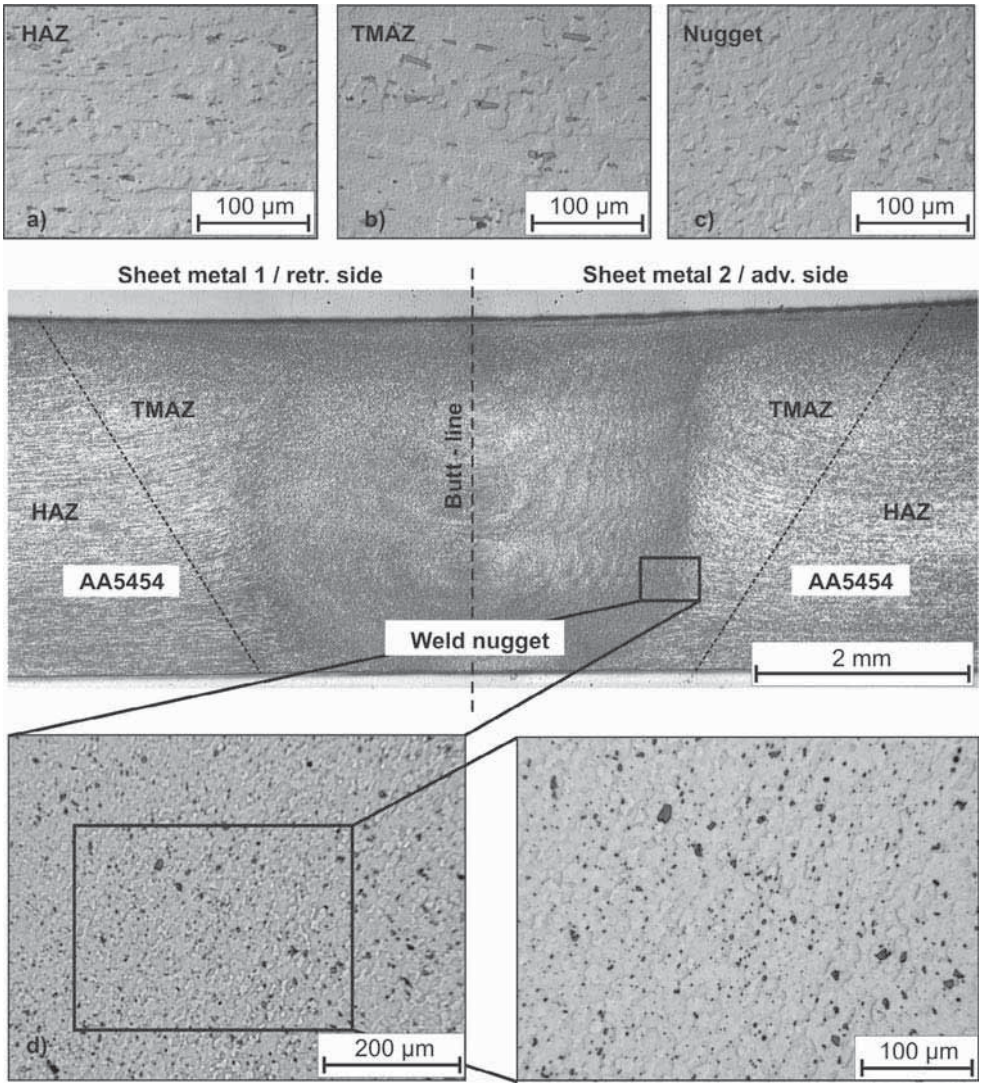

Figure 5 – Light micrograph of a AA5454 FSW-joint with details of HAZ, TMAZ and nugget as well as borderline between nugget and TMAZ

in recrystallized condition without a preferential grain orientation [15, 16]. The grain size of about 5-10 µm is significantly lower compared to the parent materials grain size. The original rolling structure does not exist any more. The border line of the nugget [Figure 5 d)] is characterized by smaller segregations in comparison to the base material as a consequence of the rotation of the welding tool [17]. This area is surrounded by the thermal mechanical affected zone (TMAZ) [Figure 5 b)] with plastic deformed, not complete recrystallized grains and farther the heat-affected zone (HAZ) [Figure 5 a)].

3.3 Micro hardness profile

For the friction stir welded AA5454-joints the influence of the welding process on the developing micro hardness profile was investigated in detail (Figure 6). The 2D-hardness profile was determined by using a

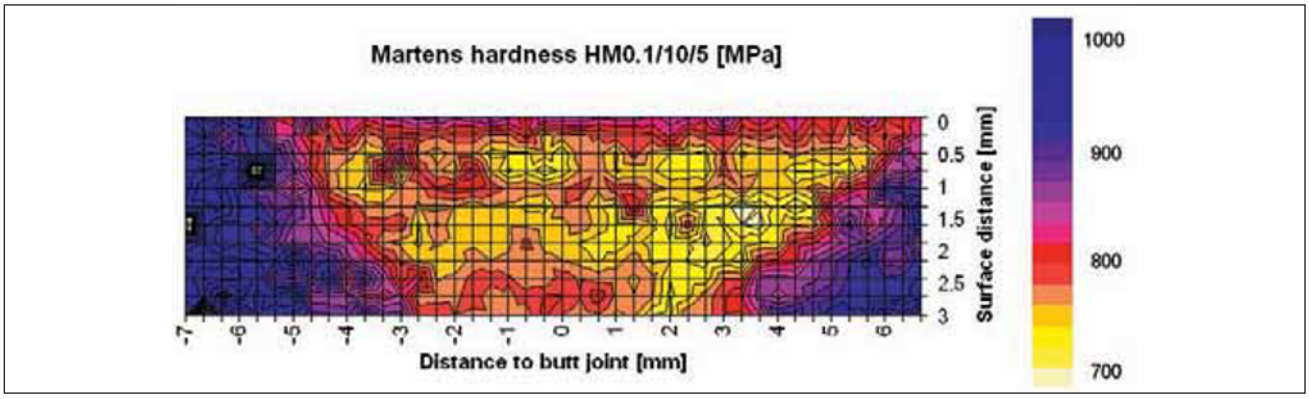

Figure 6 – Martens hardness profile of the cross-section of a AA5454 FSW-joint

Fischerscope. In the area of the weld nugget and the TMAZ a significant hardness decrease is observable. The base material shows a martens hardness of about 1000 MPa whereas the hardness of the TMAZ and the weld nugget is decreased to a minimum of about 700 MPa as a result of partly recrystallized microstructure in this area. The trapezoidal expansion of the softened area is caused by the special geometry of the welding tool. The hardness reduction leads to reduced monotonic and cyclic strength of the welded joints for the investigated Al-alloy.

3.4 Monotonic loading

Stress-strain-curves were measured for the base material AA5454 and corresponding FSW-joints (Figure 7). The resulting tensile strength of the friction stir welded A5454/A5454-joint with 267 MPa achieves 90 % of the strength of the base material. The yield strength $R_{p0.2}$ of the friction stir welded joint decreases from 220 MPa to 135 MPa in the welding zone. With about 18 % the elongation of the joint attains a considerable higher value in comparison to the base material. The fine grained microstructure in the welding area provides a high deformation capability. The small increases and decreases in the progression of both curves can be related to the Portevin-LeChatelier (PLC) effect which is typical for this material.

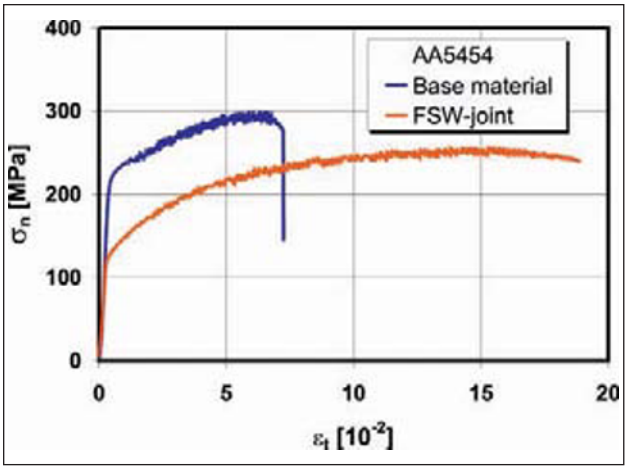

Figure 7 – Monotonic stress-strain curves of the AA5454 base material and FSW-joint

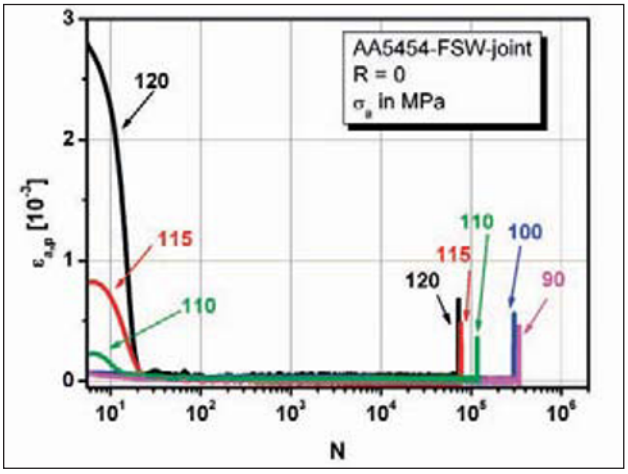

Figure 8 – Cyclic deformation curves of FSW-joints

3.5 Cyclic loading

In Figure 8 the cycle-dependent course of the plastic strain amplitude is plotted for stress amplitudes between 90 and 120 MPa. The cyclic deformation behaviour of the welding zone is characterized by pronounced cyclic hardening within the first 20 cycles leading to plastic strain amplitudes nearby zero until macro-crack growth. With increasing stress amplitude the plastic strain amplitude at test beginning increases and consequently the lifetime decreases from $33 \cdot 10^4$ for σ_a = 90 MPa to $7.2 \cdot 10^4$ for σ_a = 120 MPa.

For the stress amplitude σ_a = 120 MPa high-precision temperature and electrical resistance measurements to characterize the cyclic deformation behaviour are compared to the plastic strain amplitude (Figure 9). The initial decrease of the change in temperature ΔT_1, ΔT_2 and ΔT_3 is caused by cyclic hardening. Thus, the development of the change in temperature is in accordance with the plastic strain amplitude. In the following the plastic strain amplitude is zero and consequently the local temperature changes decrease to minimum values. The differing development of ΔT_1, ΔT_2 and ΔT_3 for N > 500 can be taken as an indicator, that the cyclic deformation behaviour is locally different in the welding zone. While ΔT_1 measured at the nugget and ΔT_2 measured at the retreating side lead to a minimum, ΔT_3 measured at the advancing side increases continuously for $N > 2 \cdot 10^4$ cycles until 0.5 K. Consequently, the subsequent fatigue failure at the advancing side can be reliably detected in a very early fatigue state after 30 % N_f with temperature measurements, while no significant change in plastic strain amplitude can be observed. Due to accumulated fatigue damage in the gauge length the change in electrical resistance reaches values of about 10.8 μΩ. The initial small decrease of ΔR is caused by the decreasing temperature due to cyclic hardening, followed by increasing values for $N > 2\ 10^4$ caused by proceeding fatigue damage until macroscopic crack growth. Thus, with the change in electrical resistance, fatigue failure can be indicated in the same early fatigue state as with the

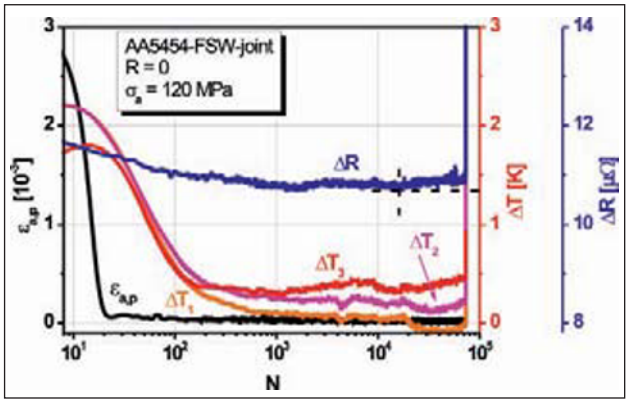

Figure 9 – Plastic strain amplitude, change in temperature and change in electrical resistance of an AA545 FSW-joint

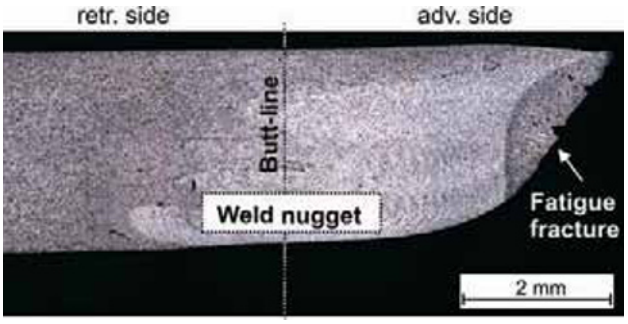

↔ *loading direction*

Figure 10 – Light micrograph of an AA5454 FSW-joint after fatigue failure

change in temperature measurements. To summarize, it can be pointed out that the changes in temperature and in electrical resistance are powerful tools to describe the actual fatigue state of FSW-joints under cyclic loading.

For the identification of the fatigue fracture position related to the friction stir weld, a light micrograph of the welding zone is shown in Figure 10. In most cases, the position of fatigue failure is located at the interface between the TMAZ and the HAZ on the advancing side of the joint (cf. Figure 5).

As shown in Figure 6, in this area the micro hardness profile shows the lowest values. Furthermore, the greatest gradient in the micro hardness profile can be observed in this area. Consequently, the proceeding fatigue failure occurs in this region, which can be interpreted as a failure initiating notch.

4 CONCLUSIONS

The tensile strength of friction stir welded AA5454-joints achieved about 90% of the tensile strength of the base material. The reduction of hardness in the welding zone, proved with a 2-D hardness profile, is combined with an enormous increase of ductility. The fatigue behaviour of AA5454-FSW-joints under constant amplitude loading can be characterized in detail by the simultaneous application of plastic strain amplitude $\varepsilon_{a,p}$, change in temperature ΔT and change in electrical resistance ΔR measurements. Temperature and electrical resistance measurements provide additional information about the actual fatigue state. The fatigue behaviour of the welding zone is characterized by pronounced cyclic hardening within the first 20 cycles, leading to plastic strain amplitudes of nearby zero until macro-crack growth. On the basis of local temperature measurements it was found that the fatigue behaviour is locally different in the welding zone. Fatigue failure can be reliably detected in a very early fatigue state after 30 % N_f on the basis of temperature measurements and electrical resistance measurements, while no significant change in plastic strain amplitude can be observed.

REFERENCES

[1] Thomas W.M., Nicholas E.D., Needham J.C., Murch M.G., Templesmith P., Dawes C. J.: Improvements relating to friction welding, Patent WO 9310935, 1992.

[2] Ilyushenko R., Nesterenkov V.: Novel technique for joining of thick section difficult-to-weld aluminium alloys, Mat. Sci. Forum, 2006, 519-521, pp. 1125-30.

[3] Thomas W.M., Nicholas E.D.: Friction Stir Welding for the transportation industries, Mater. Des., 1997, 18, pp. 269-73.

[4] Schneider J., Beshears R., Nunes A. C.: Interfacial stikking and slipping in the friction stir process, Mat. Sci. Eng. A, 2006, 435-436, pp. 297-304.

[5] Kallee S.W., Kell J.M., Thomas W.M., Wiesner C.S.: Development and implementation of innovative joining processes in the automotive industry, DVS Annual Welding Conf., Essen, 2005.

[6] Johnsen M.R.: Friction Stir Welding takes off at Boeing, Weld. J., 1999, 78, pp. 35-39.

[7] Aronson R.B.: A new look at aircraft assembly, Friction Stir Welding is the answer, Manuf. Eng., 2004 132.

[8] Walther F., Eifler D.: Cyclic deformation behavior of steels and light-metal alloys, Mat. Sci. Eng. A, 2007, 468-470, pp. 259-66.

[9] Rojek N., Smaga M., Walther F., Eifler D.: Cyclic deformation behavior and lifetime calculation of AlMg3Mn, Mat.-wiss. u. Werkstofftech., 2007, 38, pp. 249-54.

[10] Biallas G., Piotrowski A., Eifler D.: Cyclic stress-strain, stress-temperature and stress electrical resistance response of NiCuMo alloyed sintered steels, Fatigue Fract. Engng. Mater. Struct., 1995, 18, pp. 605-615.

[11] Frankel G.S., Xia Z.: Localized Corrosion and stress corrosion cracking resistance of Friction Stir Welded aluminium alloy 5454. Corrosion, 55, pp. 139-50, 1999.

[12] Lee H.T., Chen J.C., Wang J.M.: Thermomechanical behaviour of metals in cyclic loading, J. Mat. Sci., 1993, 28, pp. 5500-07.

[13] Wagner G., Gutensohn M., Eifler D.: Monotonic properties and cyclic deformation behavior of Friction Stir Welded Mg/Mg-, Mg/Al- and Al/Al-joints, Magnesium Proceedings of the 7th Int. Conf. on Magnesium Alloys and Their Applications, Ed: K. U. Kainer, 2006, pp. 1092-98.

[14] Krishnan K.N.: On the formation of onion rings in Friction Stir Welds, Mat. Sci. Eng. A, 2002, 327, pp. 246-51.

[15] Sato Y., Kokawa H.: Microstructural factors governing mechanical properties in Friction Stir Welds, Key Eng. Mat., 2007, 345-346, pp. 1493-96.

[16] Fratini L., Buffa G., Palmeri D., Hua J., Shivpuri R.: Material flow in FSW of AA7075-T6 butt joints: Continuous dynamic recrystallization phenomena, J. Eng. Mater.-T., 2006, 128, pp. 428-35.

[17] Jata K.V., Sankaran K.K., Ruschau J.: Friction Stir Welding effects on microstructure and fatigue of aluminium alloy 7050-T7451, Metall. Mater. Trans., 2000, 31, pp. 2181-92.